

Handbook for Efficiently Quantifying Robustness of Magic

Hiroki Hamaguchi¹, Kou Hamada¹, and Nobuyuki Yoshioka^{2,3,4}

¹Department of Mathematical Engineering and Information Physics, University of Tokyo, 7-3-1 Hongo, Bunkyo-ku, Tokyo 113-8656, Japan

²Department of Applied Physics, University of Tokyo, 7-3-1 Hongo, Bunkyo-ku, Tokyo 113-8656, Japan

³Theoretical Quantum Physics Laboratory, RIKEN Cluster for Pioneering Research (CPR), Wako-shi, Saitama 351-0198, Japan

⁴JST, PRESTO, 4-1-8 Honcho, Kawaguchi, Saitama, 332-0012, Japan

The nonstabilizerness, or magic, is an essential quantum resource to perform universal quantum computation. Robustness of magic (RoM) in particular characterizes the degree of usefulness of a given quantum state for non-Clifford operation. While the mathematical formalism of RoM can be given in a concise manner, it is extremely challenging to determine the RoM in practice, since it involves superexponentially many pure stabilizer states. In this work, we present efficient novel algorithms to compute the RoM. The crucial technique is a subroutine that achieves the remarkable features in calculation of overlaps between pure stabilizer states: (i) the time complexity per each stabilizer is reduced exponentially, (ii) the space complexity is reduced superexponentially. Based on this subroutine, we present algorithms to compute the RoM for arbitrary states up to $n = 7$ qubits on a laptop, while brute-force methods require a memory size of 86 TiB. As a byproduct, the proposed subroutine allows us to simulate the stabilizer fidelity up to $n = 8$ qubits, for which naive methods require memory size of 86 PiB so that any state-of-the-art classical computer cannot execute the computation. We further propose novel algorithms that utilize the preknowledge on the structure of target quantum state such as the permutation symmetry of disentanglement, and numerically demonstrate our state-of-the-art results for copies of magic states and partially disentangled quantum states. The series of algorithms constitute a comprehensive ‘‘handbook’’ to scale up the computation of the RoM, and we envision that the proposed technique applies to the computation of other quantum resource measures as well.

1 Introduction

Universal fault-tolerant quantum computation is often formulated such that the elementary gates consist of both classically simulatable gates and costful gates, such as in the most

Hiroki Hamaguchi: hamaguchi-hiroki0510@g.ecc.u-tokyo.ac.jp

Kou Hamada: zkouaaa@g.ecc.u-tokyo.ac.jp

Nobuyuki Yoshioka: nyoshioka@ap.t.u-tokyo.ac.jp

well-known Clifford+ T formalism of the magic state model [1, 2, 3, 4, 5, 6]. Since the consumption of the non-Clifford gates is indispensable for any quantum advantage [7, 8, 9, 10], there is a surging need to evaluate the complexity of quantum circuits using the framework of resource theory, in order to explore the boundary of quantum and classical computers [11, 12, 13, 14, 15, 16, 17]. One such attempt is the proposal of a quantity called the Robustness of Magic (RoM) by Howard and Campbell [18, 19, 20]; the RoM characterizes the classical simulation overhead or complexity of a given quantum state based on its effective amount of magic, and it geometrically quantifies the distance from the convex set of stabilizer states.

The computation of the RoM can be reduced to a simple L^1 norm minimization problem. Meanwhile, since the size of the set of pure stabilizer states grows superexponentially with the number of qubits, both the time and space complexity are prohibitively large, so it is extremely challenging to perform computation beyond $n > 5$ qubits. Concretely, the memory consumption blows up to 86 PiB even for $n = 8$ qubit system. Existing works have been done to offload such a heavy burden; for instance, Ref. [20] proposed to utilize the symmetry of the target state. By exploiting the permutation symmetry between copies of identical states and also the internal (or local) symmetry, it has been shown that, if one considers copies of symmetric magic states such as $|H\rangle^{\otimes n}$ used for T -gates, one can simulate up to $n = 26$ qubits. However, when one is interested in the magic resource of noisy states, for instance, there is no valid way to scale up the characterization of the resource.

In this work, we propose a systematic procedure as shown in Fig. 1 to compute the RoM value that overcomes the barrier in the existing works. Central to our work is the subroutine that computes the overlaps of a given quantum state between stabilizer states with (i) exponentially faster time complexity per stabilizer state (ii) superexponentially smaller space complexity. Using this efficient subroutine, we propose algorithms that surpass the state-of-the-art results of the RoM calculation for arbitrary states up to $n = 7$ qubits. We also extend the capability of methods that utilize the preknowledge of the target quantum states such as the permutation symmetry and decoupled structure, and show that we may compute the RoM for multiple copies of arbitrary single qubit states up to $n = 17$ qubits.

The remainder of this work is organized as follows. In Sec. 2, we present the preliminaries regarding the formalism of RoM. In Sec. 3, we first give the main subroutine on the overlap calculation (Theorem 1), and then present the algorithms that computes the RoM value with reduced computational resource by utilizing the information of all the overlap values between the target state and stabilizer states. In Sec. 4, we present algorithms for practical target states that are decoupled from each other, such as the multiple copies of single-qubit states or tensor products over subsystems. Finally, in Sec. 5, we provide the discussion and future perspective of our work.

2 Preliminaries

2.1 Robustness of magic

Let $\mathcal{P}_n = \{\pm 1, \pm i\} \times \{I, X, Y, Z\}^{\otimes n}$ be the n -qubit Pauli group. For any n -qubit stabilizer state $|\psi\rangle$, we denote by $\text{Stab}(|\psi\rangle) = \langle P_1, \dots, P_n \rangle$ the stabilizer group of $|\psi\rangle$, i.e., the group generated by the set of n independent Pauli operators such that $P_i |\psi\rangle = |\psi\rangle$ for each generator P_i . We denote the entire set of n -qubit stabilizer states as \mathcal{S}_n , whose size scales superexponentially as $|\mathcal{S}_n| = 2^n \prod_{k=0}^{n-1} (2^{n-k} + 1)$ [21, 22], and also denote the convex hull of them as $\text{STAB}_n = \{\sum_i p_i \sigma_i \mid \sigma_i \in \mathcal{S}_n, p_i \geq 0, \sum_i p_i = 1\}$.

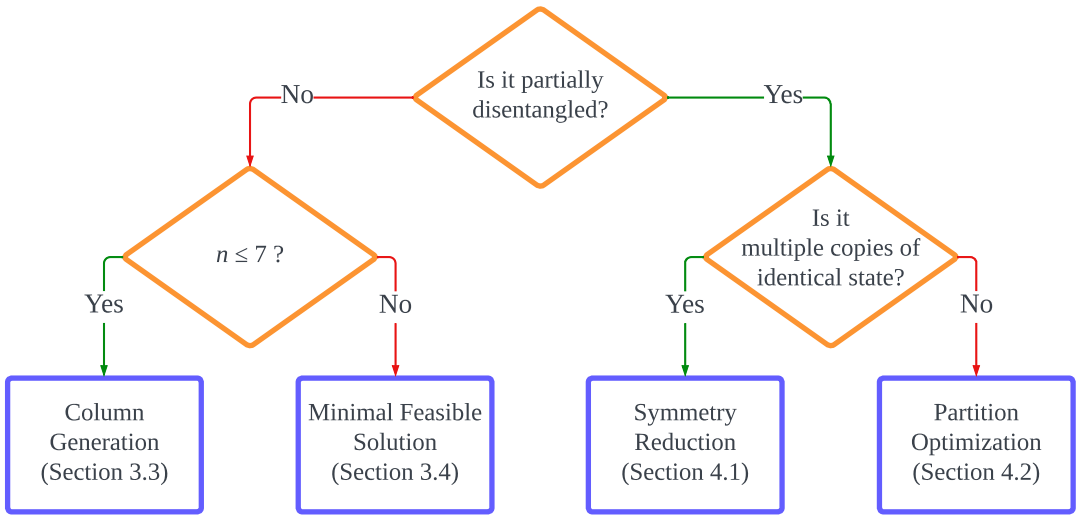


Figure 1: Flow chart of RoM computation.

Method	Target	Qubit count	Exact/Approximate
Brute-force LP [18]	Arbitrary	$n \leq 5$	Exact
Top-overlap	Arbitrary	$n \leq 7$	Exact*
Column Generation (CG)	Arbitrary	$n \leq 7$	Exact
Minimal Feasible Solution	Arbitrary	$n \leq 14$	$2^{n/2}$ -approximation
Symmetry Reduction	$\rho^{\otimes n}$	$n \leq 17$	Exact up to $n \leq 7$
Partition Optimization	$\bigotimes_i \rho_i$	$n \leq 15$	Approximation
Symmetry Reduction [20]	$\rho_{H,F}^{\otimes n}$	$n \leq 26$	Exact up to $n \leq 9, 10$

Table 1: Methods for calculating RoM. The top four methods are applicable to arbitrary n -qubit states, while the latter three assume certain structures such as permutation symmetry, decoupled structure, and local symmetry. The expression ‘Exact*’ is intended to denote that there is a hyperparameter that controls the accuracy of the solution, while we have performed numerical demonstrations that successfully find the exact solution.

The Robustness of Magic (RoM) of a given n -qubit quantum state ρ is defined as the distance from the polytope of the free states identified with STAB_n as [18, 23]

$$\mathcal{R}(\rho) := \min_{\sigma_+, \sigma_- \in \text{STAB}_n} \left\{ 2p + 1 \mid \rho = (p+1)\sigma_+ - p\sigma_-, p \geq 0 \right\}. \quad (1)$$

It is straightforward to show that this yields an equivalent expression as

$$\mathcal{R}(\rho) = \min_{\mathbf{x}} \left\{ \sum_{i=1}^{|\mathcal{S}_n|} |x_i| \mid \rho = \sum_{\sigma_i \in \mathcal{S}_n} x_i \sigma_i, x_i \in \mathbb{R} \right\}, \quad (2)$$

which can be further simplified as

$$\mathcal{R}(\rho) = \min_{\mathbf{x}} \left\{ \sum_{i=1}^{|\mathcal{S}_n|} |x_i| \mid \mathbf{A}_n \mathbf{x} = \mathbf{b} \right\}. \quad (3)$$

Here, we have utilized the unique decomposition of the quantum state into n -qubit Pauli operators to define $b_j = \text{Tr}[\rho P_j]$ and $(\mathbf{A}_n)_{j,i} = \text{Tr}[\sigma_i P_j]$ where P_j ($1 \leq j \leq 4^n$) is the

j -th Pauli operator. Here, \mathbf{A}_n encapsulates the information of the entire pure stabilizer states, whereas \mathbf{x} stores that of the target quantum state ρ . It is also convenient to define $\mathcal{A}_n = \{\mathbf{a}\}$ as the entire set of columns in \mathbf{A}_n such that $\mathbf{A}_n = (\mathbf{a})_{\mathbf{a} \in \mathcal{A}_n}$. In practice, one may solve Eq. (3) as a linear programming (LP) as follows:

$$\begin{aligned} & \underset{\mathbf{u}}{\text{minimize}} \quad \sum_i u_i \\ & \text{subject to} \quad (\mathbf{A}_n \quad -\mathbf{A}_n) \mathbf{u} = \mathbf{b}, \\ & \quad \mathbf{u} \geq \mathbf{0}, \end{aligned} \tag{4}$$

where the inequality denotes the element-wise inequality. For the sake of convenience for later discussion, we denote a function $\text{SolveLP}(\mathcal{A}, \mathbf{b})$ that returns $\mathcal{R}(\rho)$ and \mathbf{x} by solving Eq. (4) given a set of columns \mathcal{A} , and also denote the minimization problem itself as $\text{Prob}(\mathbf{A}, \mathbf{b})$ using the matrix determined from the set \mathcal{A} .

2.2 Dualized Robustness of Magic

Since the RoM can be formalized via the LP, the strong duality holds, which implies that the dual problem gives an equivalent definition. Concretely, the value of the RoM can be computed via the following:

$$\mathcal{R}(\rho) = \max_{\mathbf{y}} \left\{ \mathbf{b}^\top \mathbf{y} \mid -\mathbf{1} \leq \mathbf{A}_n^\top \mathbf{y} \leq \mathbf{1} \right\}, \tag{5}$$

where $\mathbf{1}$ is a length- 4^n vector with all the elements given by unity. By the nature of the dual problem, any feasible solution yields a lower bound on the RoM. For instance, it can be shown by taking $\mathbf{y} = (\dots, \text{sgn}(\text{Tr}[\rho P_j])/2^n, \dots)$ that, the RoM can be lower-bounded by the st-norm as $\|\rho\|_{\text{st}} = \frac{1}{2^n} \|\mathbf{b}\|_1$ [20].

3 Scaling up RoM calculation for arbitrary states

It is known that LP can be solved with polynomial complexity with respect to the matrix size. However, it must be noted that the matrix size of \mathbf{A}_n is $4^n \times |\mathcal{S}_n|$ where $|\mathcal{S}_n| = 2^{\mathcal{O}(n^2)}$, and hence it is impractical to use the brute-force solver to tackle $n > 5$ qubit systems [14].

Motivated by such a problematic situation, we propose two numerical algorithms that compute the RoM for arbitrary quantum states beyond the state-of-the-art system size. The key technique is to utilize a subroutine that achieves the following two remarkable features in overlap calculation: (i) total time complexity is drastically improved from $\mathcal{O}(2^n |\mathcal{S}_n|)$ to $\mathcal{O}(n |\mathcal{S}_n|)$, which is due to the exponential reduction from $\mathcal{O}(2^n)$ to $\mathcal{O}(n)$ per stabilizer state, (ii) the space complexity is reduced superexponentially from $\mathcal{O}(2^n |\mathcal{S}_n|)$ to $\mathcal{O}(2^n)$ since we do not explicitly construct the entire \mathbf{A}_n . Based on such a subroutine, the first algorithm referred to as the top-overlap method (Algorithm 1) solves the primal problem (3) with a limited set of stabilizers whose overlap with the target quantum state is taken from largest or smallest ones. The second algorithm referred to as the Column Generation method (Algorithm 2), on the other hand, iteratively adds stabilizer states for the decomposition until all the inequality constraints in the dual problem (5) are satisfied, such that one has a guarantee for the exact solution.

In the following, we first present the fast overlap computation algorithm in Sec. 3.1, and then proceed to introduce two novel algorithms in Sec. 3.2 and 3.3, respectively. We show that these algorithms enable us to compute the exact RoM value up to $n = 7$ qubit

system. In this case, the memory consumption for the main subroutine is suppressed by a factor of 10^5 ; compared to 86 TiB required by brute-force methods, we can run the efficient subroutine with only 499 MiB.

3.1 Core subroutine: fast computation of stabilizer overlaps

First, we introduce the core subroutine for computing the overlaps of the target state and pure stabilizer states, which are referred to as the stabilizer overlaps in the following. Note that computing the overlaps with the matrix-vector product of $\mathbf{A}_n^\top \mathbf{y}$ for n -qubit system requires time complexity of $\mathcal{O}(4^n |\mathcal{S}_n|)$ if we resort to naive computation. Even if we utilize the sparsity of \mathbf{A}_n , the cost is still $\mathcal{O}(2^n |\mathcal{S}_n|)$. We show that this can be done exponentially faster with n for each stabilizer state:

Theorem 1. *(Complexity of computing all stabilizer overlaps) Computation of $\mathbf{A}_n^\top \mathbf{y}$ can be done in time complexity of $\mathcal{O}(n |\mathcal{S}_n|)$ and space complexity of $\mathcal{O}(2^n)$.*

One of the most practical applications of this theorem is to apply to the computation of overlaps $\mathbf{A}_n^\top \mathbf{b}$ for the Pauli vector \mathbf{b} of a given quantum state; as we later detail in Sec. 3.2, this technique is essential to scale up the RoM calculation to larger systems.

In order to show Theorem 1, first we introduce the Fast Walsh–Hadamard Transform (FWHT) algorithm that efficiently performs matrix-vector product operation, when there is a tensor product structure in the matrix [24]. Here we define the unnormalized Walsh–Hadamard matrix as $H_n := H^{\otimes n}$ where $H := \begin{pmatrix} 1 & 1 \\ 1 & -1 \end{pmatrix}$. As is evident from the well-known pseudocode provided in Appendix A, we can show the computational cost is given as the following lemma:

Lemma 1. *(Complexity of FWHT algorithm) Matrix-vector multiplication of Walsh–Hadamard matrix can be done by in-place computation with time complexity of $\mathcal{O}(n 2^n)$ and space complexity of $\mathcal{O}(2^n)$ using the FWHT algorithm.*

Next, we show that \mathbf{A}_n is essentially constructed by a concatenation of Walsh–Hadamard matrices (see also Fig. 2). Let \mathcal{W}_n denote a set of all matrices that can be expressed as sparsified form of $\begin{bmatrix} H_n \\ O \end{bmatrix}$ by reordering and flipping the signs of the rows appropriately, where O denotes a null matrix of size $(4^n - 2^n) \times 2^n$. We can state the following lemma (see Appendix D for the proof):

Lemma 2. *(Decomposition of \mathbf{A}_n into Walsh–Hadamard matrix) For all $n \in \mathbb{N}$, there exists a constructive and efficient way of enumerating properly sparsified Walsh–Hadamard matrices $\{W_j\}_{j=1}^{|\mathcal{S}_n|/2^n}$ ($W_j \in \mathcal{W}_n$) such that*

$$\mathbf{A}_n = [W_1 \cdots W_{|\mathcal{S}_n|/2^n}]. \quad (6)$$

By combining Lemma 1 and 2, we complete the proof of Theorem 1. As a direct corollary, we also obtain that the stabilizer fidelity defined as $F_{\text{STAB}}(|\psi\rangle) = \max_{|\phi\rangle \in \mathcal{S}_n} |\langle \psi | \phi \rangle|^2$ [25] can be shown to be computed exponentially faster as well (see Appendix B for details):

Corollary 1. *(Complexity of computing stabilizer fidelity) Stabilizer fidelity can be computed with time complexity of $\mathcal{O}(n |\mathcal{S}_n|)$ and space complexity of $\mathcal{O}(2^n)$.*



Figure 2: Visualization of A_n for $n = 1$ and $n = 2$.

Qubit count n	Full size	Our work
4	3 MiB	301 KiB
5	379 MiB	4 MiB
6	95 GiB	97 MiB
7	86 TiB	499 MiB
8	86 PiB	<5 GiB

Table 2: Memory size required to store the reduced A of column size fraction K that is taken as the values mentioned in Sec. 3.2. The proposed methods do not explicitly construct the entire A_n but compute all overlaps from in-place computation. The data is based on sparse matrix format in SciPy [26]. The code for generating A_n and proposed algorithms are available via GitHub [27].

It has been recognized that the stabilizer fidelity cannot be computed with moderate computational cost for $n > 5$ [14], while our algorithm allows us to compute up to $n = 8$ with significantly reduced space complexity in approximately two days, using a *laptop* with 11th Gen Intel(R) Core(TM) i5-1135G7 CPU and 16.0 GB RAM. For concrete values of the memory consumption, see Table 2.

3.2 Top-overlap method for primal RoM

Using the efficient overlap calculation algorithm presented in Sec. 3.1, we propose a novel algorithm that computes the exact/approximate value based on the following: (i) by the nature of L^1 norm minimization problem, the solution of the optimal stabilizer decomposition is sparse [28], (ii) the stabilizer overlap is closely related with the optimal stabilizer decomposition (see Fig. 3 (a)). Concretely, as we provide the detail in Algorithm 1, we restrict the number of columns in A_n and consider only a fraction of pure stabilizer states with largest or smallest overlaps.

As a useful visualization to confirm (ii), in Fig. 3(a) we show the distribution of stabilizer overlap $\{\text{Tr}[\rho\sigma_i]\}_i$ and their weights $\{x_i\}_i$ for random 4-qubit mixed state $\rho = \sum_{\sigma_i \in \mathcal{S}_n} x_i \sigma_i$. Indeed, we find strong correspondence between the overlaps and the weights, and observe that the similar property can be seen in various random instances in larger systems as well.

It is natural that stabilizer states with large overlaps have large weights. On the other hand, it seems quite counterintuitive that stabilizer states with small overlaps contribute non-negligibly. In this regard, we mention that in the field of operations research, there is an approximation method called Orthogonal Matching Pursuit for L^1 norm minimization problem that greedily takes near-orthogonal basis to improve the solution [29, 30]. In a sense, orthogonal bases contribute to extending the effective dimension of the space spanned by the chosen basis, and thus are essential for the current problem to enhance the

Algorithm 1: Top-overlap method for primal RoM

Input: Pauli vector \mathbf{b} for quantum state ρ ,
 Fraction K ($0 < K \leq 1$)

Output: Approximate RoM

- 1 Compute overlap $\mathbf{a}^\top \mathbf{b}$ for each $\mathbf{a} \in \mathcal{A}_n$ using FWHT algorithm
- 2 $\mathcal{C} \leftarrow$ Partial column set $\{\mathbf{a}\}$ with $K|\mathcal{S}_n|$ largest and smallest overlaps
- 3 **return** $\text{SolveLP}(\mathcal{C}, \mathbf{b})$

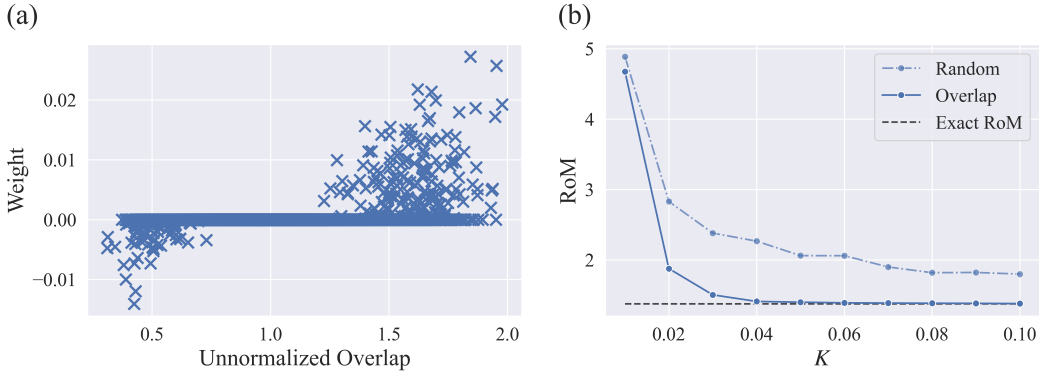


Figure 3: (a) Stabilizer overlaps $\text{Tr}[\rho \sigma_i]$ and the weights x_i for random mixed state of $n = 4$ qubits. (b) RoM value computed under restricted set of stabilizers of ratio $0 < K \leq 1$ for random mixed state of $n = 4$ qubits.

quality of the approximation for random states. As we discuss in Sec. 4, the number of bases is significantly reduced for tensor product states whose symmetry can be exploited.

As we highlight in Fig. 3(b), we only need a small fraction from the entire \mathcal{S}_n in order to obtain a nearly-exact solution. We find that, for a random mixed state of $n = 4$ qubit system, it is sufficient to use a fraction of $K \sim 0.05$ in order to achieve an absolute error of 0.023. We empirically find that $K = 10^{-n+3}$ is sufficient for $4 \leq n \leq 6$, and it is even suppressed as $K = 10^{-5}$ for $n = 7$ to obtain similar accuracy. Meanwhile, we remark that we must take significantly larger column set to assure the exact RoM value; the fraction is $K \sim 0.32$ for $n = 4$ qubit case, which is increased by a magnitude of order. We provide further numerical details in Appendix H.1.

3.3 Column generation method for dualized RoM

Despite the significant improvement over brute-force methods, there are three major issues in Algorithm 1: (i) we cannot tell whether the partial column set $\mathcal{C} \subset \mathcal{A}_n$ is sufficient to yield the exact solution, (ii) there is no quantitative measure to judge the quality of the approximate solution, (iii) there is a large gap in the computational resource between ‘highly approximate’ and ‘exact’ solutions. While we do not address these problems explicitly for the primal formulation of RoM, we find that these issues are well addressed when we consider the dualized formalism instead.

Recall that the dualized formulation of RoM is given as

$$\mathcal{R}(\rho) = \max_{\mathbf{y}} \left\{ \mathbf{b}^\top \mathbf{y} \mid -\mathbf{1} \leq \mathbf{A}_n^\top \mathbf{y} \leq \mathbf{1} \right\}. \quad (7)$$

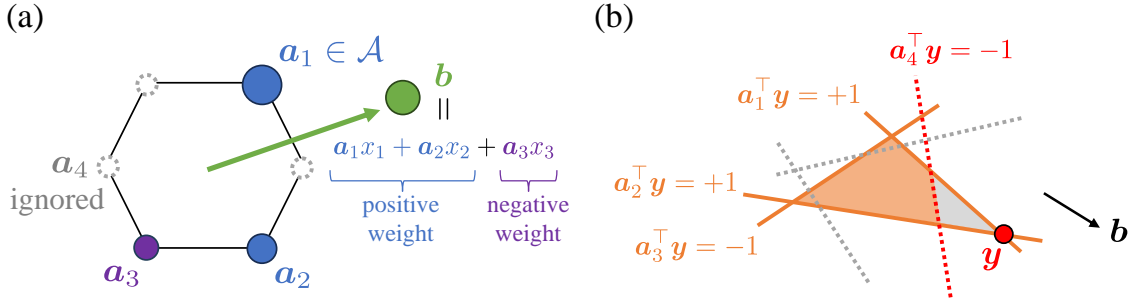


Figure 4: (a) Graphical description of the primal formalism for the RoM. The Pauli vector b of the target state is decomposed into a sum over those of pure stabilizer states a denoted by vertices on the stabilizer polytope, so that the L^1 norm of primal variables $\|x\|_1$ is minimized. The restriction on columns of A_n is expressed by gray vertices that are eliminated from the decomposition. (b) Graphical description of the dual formalism for the RoM. The equality constraints in primal problem are now given as inequalities $-1 \leq A_n^\top y \leq 1$ for the dual variables y , while the objective function is the inner product with b . A solution y obtained from reduced column set \mathcal{C} may violate some constraints, denoted by the red dotted line in the figure, so that one shall add more columns to improve the solution, while there are some columns denoted by gray dotted lines that do not affect the result.

Algorithm 2: Exact dual RoM calculation by Column Generation

Input: Pauli vector b of target state ρ
Output: Exact RoM $\mathcal{R}(\rho)$

- 1 $\mathcal{C} \leftarrow$ Partial set of \mathcal{A}_n /* Initialize using top and least overlaps */
- 2 **while** *true* **do**
- 3 $R, y \leftarrow \text{SolveLP}(\mathcal{C}, b)$
- 4 $\mathcal{C}' \leftarrow \{a \in \mathcal{A}_n \mid |a^\top y| > 1\}$ /* Use of FWHT */
- 5 **if** $\mathcal{C}' = \emptyset$ **then**
- 6 **break**
- 7 $\mathcal{C} \leftarrow \mathcal{C} \cup \mathcal{C}'$
- 8 **return** R

Let us assume that we have computed the RoM under a restricted column set \mathcal{C} , and that the solver has returned a dual variable \hat{y} , which is often the case for practical implementations. If \hat{y} does not obey all the constraints in Eq. (7), i.e., if there exists $a \in \mathcal{A}_n$ such that $|a^\top \hat{y}| > 1$, then we must increase the size of the reduced column set \mathcal{C} to include violated a 's if we wish to obtain the exact value of the RoM (see also Fig. 4). Conversely, when there is no violation, then the solution is exact, due to the strong duality of the LP.

This discussion naturally motivates us to employ an iterative method that gradually takes constraints into account until there is no violation of the constraints at all. Such a strategy is known as the Column Generation technique in the field of operations research [31], and here we propose a method that unifies the knowledge of such technique and the FWHT algorithm introduced in Sec. 3.2. Namely, as we detail in Algorithm 2, we use the FWHT algorithm as in Theorem 1 to compute the overlap $a^\top \hat{y}$ for every $a \in \mathcal{A}_n$ at each iteration, whose complexity is reduced from $\mathcal{O}(2^n |\mathcal{S}_n|)$ to $\mathcal{O}(n |\mathcal{S}_n|)$. By extending \mathcal{C} until there is no violation, we obtain the exact RoM. Note that it is practically beneficial in terms of suppressing $|\mathcal{C}|$ to introduce a threshold d ($0 \leq d \leq 1$) to discard columns a_i that satisfy both $|a_i^\top \hat{y}| < d$ and $x_i = 0$, where x_i is the corresponding primal variable.

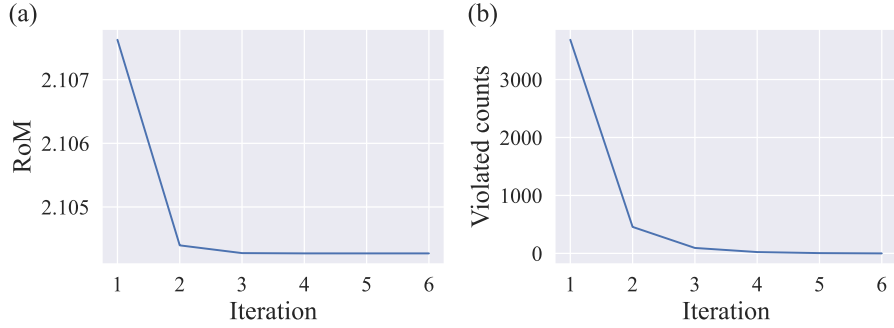


Figure 5: Demonstration of Algorithm 2 for random mixed state of $n = 7$ qubits. The number of violated columns becomes zero after 6 iterations, which assures that the exact RoM value is obtained. The first iteration is computed using the column set obtained from overlap calculation for $K = 10^{-5}$.

In Fig. 5, we present the results of the numerical demonstration of Algorithm 2. We have initialized the partial column set with a fraction of $K = 10^{-5}$ for a random mixed state of $n = 7$ qubit system, and find that the exact solution can be obtained after only 6 iterations. While we cannot derive a nontrivial bound on the number of columns used in the Column Generation technique, we observe that the thresholding technique significantly suppresses the number of unnecessary columns, such that the first iteration with a fraction of K gives the maximal memory consumption.

We empirically find that in similar to the case in Sec. 3.2, the algorithm with fraction $K \sim 10^{-n+3}$ works successfully for $4 \leq n \leq 6$, while it is an open problem whether such a heuristic choice can be justified. By using smaller values of K , one may speed up the early stage of the iteration, while we have experienced an overwhelmingly large number of violated columns such that the run time does not benefit as a total. A similar effect is also observed when we choose an inappropriately large threshold d ; the matrix size is small at early stages, while we observe an increase in violation columns so that the total run time blows up.

3.4 Minimal feasible solution with accuracy guarantee

Exact solutions for large-scale systems may require prohibitively large computational resources, while we may still wish to compute a feasible solution. Here, we propose a method with minimal computational resources that is always guaranteed to yield a feasible solution.

A technical contribution of this section is the construction of a reduced \mathbf{A} matrix that always guarantees a feasible decomposition of ρ into stabilizer states. While we guide readers for the proof to Appendix E, here we simply provide the core proposition:

Proposition 1. *(Existence of cover stabilizer set)* Let S_n be a subset of \mathcal{S}_n such that, for any $P \in \mathcal{P}_n$ there exists $|\psi\rangle \in S_n$ that satisfies $\{P, -P\} \cap \text{Stab}(|\psi\rangle) \neq \emptyset$. Then, for all $n \in \mathbb{N}$, the size of the set is bounded as $|S_n| \geq 2^n + 1$, and one can construct S_n such that $|S_n| = 2^n + 1$.

Using this proposition, it is straightforward to see that the following theorem holds:

Theorem 2. *(Existence of cover matrix)* Let $S_n = \{|\psi_j\rangle\}_j$ be a minimal cover stabilizer set that is obtained from Proposition 1. Let the stabilizer group denoted as $\text{Stab}(|\psi_j\rangle) = \langle Q_1^{(j)}, \dots, Q_n^{(j)} \rangle$, and let $|\psi_{j,\chi}\rangle$ be defined for $\chi = (\chi_1, \dots, \chi_n) \in \{0, 1\}^n$ so that $\text{Stab}(|\psi_{j,\chi}\rangle) = \langle (-1)^{\chi_1} Q_1^{(j)}, \dots, (-1)^{\chi_n} Q_n^{(j)} \rangle$, and $\mathbf{a}_{j,\chi}$ be its Pauli vector. Then, by defining $M :=$

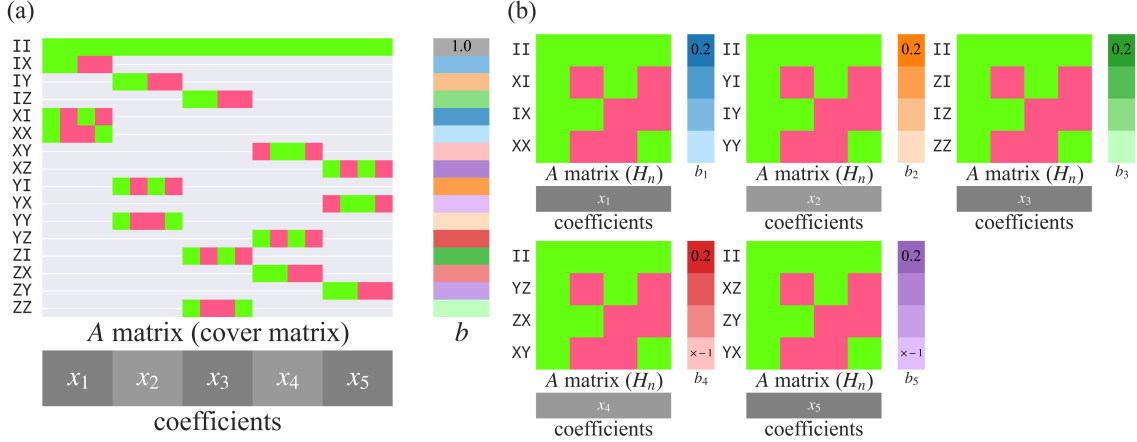


Figure 6: Graphical description of (a) the cover matrix and (b) application of FWHT algorithm for individual segments.

($\dots, \mathbf{a}_{j,\chi}, \dots$), it is guaranteed that there exists a feasible solution to $\text{Prob}(M, \mathbf{b})$ that can be solved with time complexity of $\mathcal{O}(n4^n)$.

Proof. The cover stabilizer set S_n is constructed so that, for any $P \in \{I, X, Y, Z\}^{\otimes n} \setminus \{I^{\otimes n}\}$, there is a unique $|\psi_j\rangle$ that satisfies $P|\psi_j\rangle \in \{|\psi_j\rangle, -|\psi_j\rangle\}$. Consequently, for all $|\psi_j\rangle \in S_n$ ($1 \leq j \leq 2^n + 1$), one may enumerate the set of indices $\mathcal{I}_j = \{\nu_j \mid P_{\nu_j}|\psi_j\rangle \in \{|\psi_j\rangle, -|\psi_j\rangle\}\}$. By extracting the elements from \mathbf{b} as $\mathbf{b}_j = (b_{\nu_j})_{\nu_j \in \mathcal{I}_j}$, the primal problem in the reduced bases is equivalent to $H_n \mathbf{x}_j = \mathbf{b}_j$ where H_n is the unnormalized Walsh–Hadamard matrix. Therefore, for each j we can simply compute by the FWHT algorithm as

$$\mathbf{x}_j = (1/2^n) H_n \mathbf{b}_j, \quad (8)$$

and then combine all the solutions to construct \mathbf{x} that is assured to be feasible by the nature of the cover stabilizer set S_n (see Fig. 6 for example in $n = 2$). Since each FWHT algorithm can be performed with time complexity of $\mathcal{O}(n2^n)$, the total time complexity is $\mathcal{O}(n4^n)$. \square

We remark that we can not only ensure feasibility by Theorem 2 but also provide an accuracy bound for the algorithm. Let R_{FWHT} be the approximate RoM value obtained from the minimal feasible solution. We can show that the following holds:

Lemma 3. (Accuracy bound of minimal feasible solution) Let \mathbf{b}_j drawn uniformly from $\mathcal{N}(\mathbf{0}, \mathbf{I})$ for all j . Then,

$$\mathbb{E}_{\mathbf{b}_j \sim \mathcal{N}(\mathbf{0}, \mathbf{I})} \left[\frac{R_{\text{FWHT}}}{\|\rho\|_{\text{st}}} \right] \approx 2^{n/2}. \quad (9)$$

We guide readers for proof to Appendix F. Note that this lemma allows us to expect that $R_{\text{FWHT}} \leq 2^{n/2} \mathcal{R}(\rho)$ for a random state with high probability at the asymptotic limit of large n , while we practically observe convergence already at $n \leq 10$ (see Appendix F). While R_{FWHT} significantly deviates from the exact RoM value, we envision that the feasible solution can be utilized as, e.g., approximate initialization.

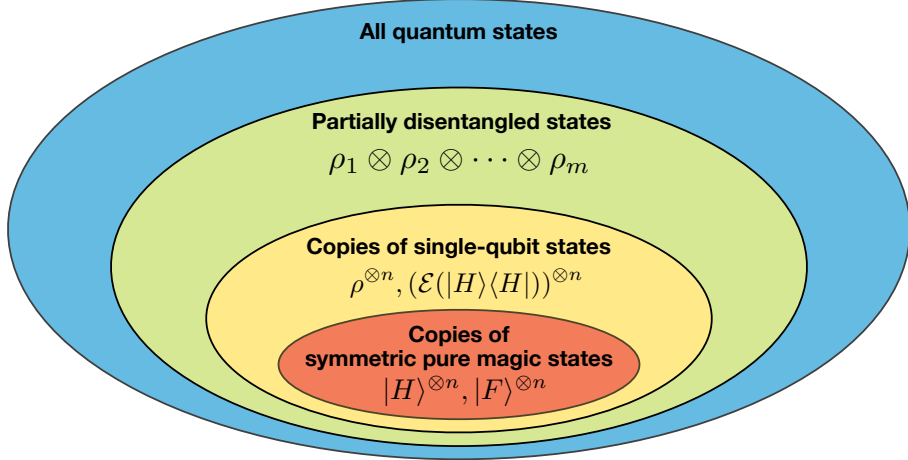


Figure 7: Hierarchy of partially disentangled quantum states.

4 Quantum resource of multiple magic states

One of the most important applications of RoM is to measure the total nonstabilizerness of multiple magic states that are decoupled from each other. For instance, one may wish to evaluate the amount of magic resources for copies of multiple states $\rho^{\otimes n}$ to estimate the upper bound on the number of generatable clean magic states. In general, this could even include situations where the quantum states are nonequivalent, such as partially decoupled states $\bigotimes_i \rho_i$. Note that there exists a previous work by Heinrich and Gross [20] that has utilized the symmetry of some pure magic states such as $|H\rangle\langle H| = \frac{1}{2} \left(I + \frac{1}{\sqrt{2}}(X + Y) \right)$ and $|F\rangle\langle F| = \frac{1}{2} \left(I + \frac{1}{\sqrt{3}}(X + Y + Z) \right)$ to scale up the simulation up to $n = 26$ qubits, we still lack a method to investigate general quantum states with partial disentangled structure (see Fig. 7).

In this section, we apply the algorithms proposed in Sec. 3 to practical problems; copies of identical quantum states $\rho^{\otimes n}$ and partially disentangled quantum states $\bigotimes_i \rho_i$. In particular, we first discuss the case of permutation symmetric state $\rho^{\otimes n}$ in Sec. 4.1, and then also consider general partially disentangled states in Sec. 4.2.

4.1 Copies of general quantum states

When the target quantum state is given as an identical copies of a quantum state as $\rho^{\otimes n}$, we may compress the size of \mathcal{A}_n by utilizing the permutation symmetry to combine multiple columns of \mathcal{A}_n . In this work, we have employed the compression method for \mathcal{A}_n proposed in Ref. [20] to define a set of permutation symmetric columns \mathcal{Q}_n . As in Ref. [20], we also make use of the data by Danielsen [32]. This enables us to run the algorithm to obtain the exact solutions for $n \leq 7$ qubits.

Beyond $n = 7, 8$ qubits, it is not realistic to obtain the exact solution even when we use \mathcal{Q}_n instead of \mathcal{A}_n . Note that \mathcal{Q}_n is the matrix given by ordering all the columns in \mathcal{Q}_n whose number of rows (and correspondingly that of \mathbf{b}) is reduced by permutation symmetry as well. Therefore, here we propose an approximate method that performs divide-and-conquer computation. As we present the details in Algorithm 3, we consider all possible decomposition of m qubits into two groups with j and k qubits ($j + k = m$), and compute the optimal stabilizer decomposition. If one has stored the solution of the LP

Algorithm 3: Approximate RoM for permutation symmetric states

Data: Compressed column set \mathcal{Q}_n of matrix \mathbf{Q}_n
Input: Positive integer n, k ($n \geq k$), Pauli vector \mathbf{b} for target state ρ
Output: Approximate RoM value R_i of $\rho^{\otimes i}$ ($i = 1, \dots, n$)

```

1 for  $i \leftarrow 1$  to  $k$  do
2    $R_i, \mathcal{C}_i \leftarrow \text{SolveLP}(\mathcal{P}_n, \mathbf{b})$ 
3 for  $i \leftarrow k + 1$  to  $n$  do
4    $\mathcal{C}' \leftarrow \emptyset$ 
5   for  $l \leftarrow 1$  to  $\lfloor i/2 \rfloor$  do
6      $m \leftarrow i - l$ 
7      $\mathcal{C}' \leftarrow \mathcal{C}' \cup \{\rho_l \otimes \rho_m \mid \rho_l \in \mathcal{C}_l, \rho_m \in \mathcal{C}_m\}$ 
8    $R_i, \mathcal{C}_i \leftarrow \text{SolveLP}(\mathcal{C}', \mathbf{b})$ 
9 return  $(R_1, \dots, R_n)$ 

```

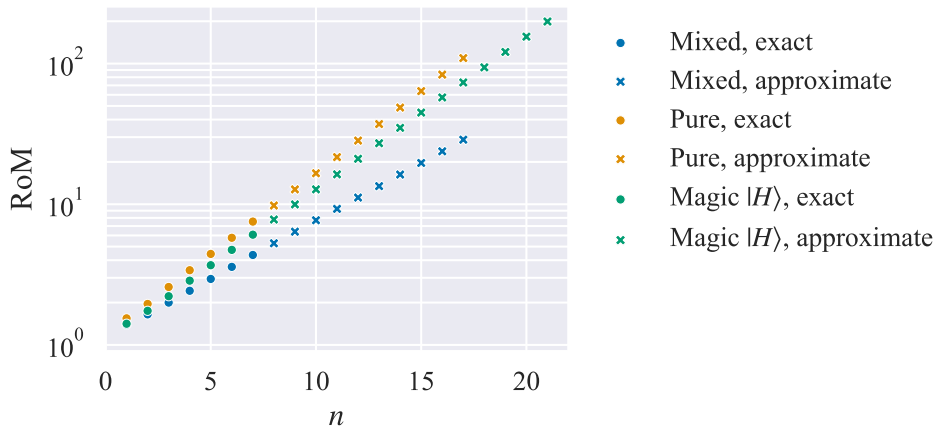


Figure 8: Exact and approximate RoM values computed for n copies of single-qubit state $\rho^{\otimes n}$. The blue, orange, and green data denote the RoM value for random mixed state, random pure state, and the magic state $|H\rangle$. The circle (crossed) points indicate that the solution is exact (approximate). The approximate values are computed from the exact solutions for $n \leq 7$ qubits.

for $\text{Prob}(\mathbf{Q}_i, \mathbf{b}_i)$ for $i < m$, one can simply load the result. We take the tensor product of stabilizers with nonzero weights as $\{\rho_j \otimes \rho_k \mid \rho_j \in \mathcal{C}_j, \rho_k \in \mathcal{C}_k\}$. By taking the union over all states to construct \mathcal{C}_m , we compute the approximate value of RoM, which is assured to be less than the product of RoMs computed for subsystems.

Figure 8 shows the results of a numerical demonstration of the proposed algorithm applied to copies of pure magic state $|H\rangle$, pure random state, and mixed random state. Using the exact stabilizer decomposition up to $k = 7$ qubits, we have successfully computed the approximate RoM value up to $n = 17$ for the pure and mixed random state, while the compressed column set size $|\mathcal{C}_n|$ is significantly smaller for $|H\rangle$ so that we have reached $n = 21$. While this is not as large as $n = 26$ reported in Ref. [20], we emphasize that the present work is based on an algorithm that is agnostic to the internal symmetry of the single-qubit state. As a remark, we mention that the approximate RoM values for copies of pure magic states are almost identical to those presented in Ref. [20]; the value was at most 1.007 times larger.

Algorithm 4: Optimization of subsystem division

Input: Target state $\rho = \bigotimes_{i=1}^m \rho_i$
 Subsystem decomposition

Output: Approximate RoM value

1 **foreach** *Decomposition of ρ_i* **do**
 2 $R_j \leftarrow \prod \mathcal{R}(\bigotimes \rho_i)$ /* Approximate RoM value for each decomposition */
 3 **return** $\min_j R_j$

4.2 Partially disentangled states

Let us assume that we are interested in a general partially decoupled state of m subsystems as $\rho = \bigotimes_{i=1}^m \rho_i$, where $\sum_{i=1}^m n_i = n$ with n_i being the qubit count of i -th subsystem and ρ_i corresponding to the local quantum state. In similar to the previous section, we may first compute the optimal decomposition for each subsystem, and then take tensor products over non-zero weight stabilizers to construct reduced basis for the total system. In this regard, we first show that assures an upper bound with small computational effort:

Proposition 2. (*Approximate RoM from multiplicativity*) *Let ρ_i be given for the i -th subsystem, $\mathcal{R}(\rho_i)$ and \mathbf{x}_i be the exact solution for $\text{Prob}(\mathbf{A}_{n_i}, \mathbf{b}_i)$. Then,*

$$R = \prod_{i=1}^m \mathcal{R}(\rho_i), \quad \mathbf{x} = \bigotimes_{i=1}^m \mathbf{x}_i, \quad (10)$$

is one of the exact solutions for $\text{Prob}(\bigotimes_{i=1}^m \mathbf{A}_{n_i}, \mathbf{b})$ where $\bigotimes_{i=1}^m \mathbf{A}_{n_i} \subset \mathbf{A}_n$

Proof. See Appendix G. □

By noting the submultiplicativity of exact RoM [18], i.e., $\mathcal{R}(\bigotimes_i \rho_i) \leq \prod_{i=1}^m \mathcal{R}(\rho_i)$, it is natural to expect that one can further improve the approximate RoM value by extending the column set from those used in $\bigotimes_{i=1}^m \mathbf{A}_{n_i}$. For instance, one may group several subsystems so that each partial LP consists of 6 or 7-qubit systems.

We find that it is more effective to consider multiple variations to divide subsystems. As we show the pseudocode in Algorithm 4, we may divide subsystems into groups so that the exact (or highly accurate approximate) value of the RoM can be computed for each group. By comparing the product of those values for various decompositions, we take the minimal value as the approximate RoM. For instance, in the case of a 15-qubit system that is decoupled into 5 subsystems as $\rho = \rho_1 \otimes \rho_2 \otimes \rho_3 \otimes \rho_4 \otimes \rho_5$, where each ρ_i is a 3-qubit state. One may compute the approximate value as $\mathcal{R}(\rho_1 \otimes \rho_2) \times \mathcal{R}(\rho_3 \otimes \rho_4) \times \mathcal{R}(\rho_5)$ or $\mathcal{R}(\rho_1) \times \mathcal{R}(\rho_2 \otimes \rho_3) \times \mathcal{R}(\rho_4 \otimes \rho_5)$, for instance, and take the minimal value as the approximate output. While there could be combinatorially many possibilities for such groupings in general, we expect that the difference is not significant when ρ_i resemble each other, e.g., when we simulate the RoM of noisy magic states. One may also speed up the computation by brute-force parallelization if needed.

5 Discussion

In this work, we have proposed a systematic procedure to compute the RoM value to surpass the state-of-the-art results for random arbitrary states, multiple copies of single-qubit magic states, and partially disentangled quantum states. We have presented a core

subroutine that is capable of computing the overlap between the target state and a pure stabilizer state with exponentially improved time complexity and superexponentially improved space complexity. Based on the efficient overlap simulation subroutine, we have proposed algorithms for arbitrary quantum states that significantly reduce the computational cost by reducing the number of stabilizer states based on the overlap values, so that RoM for $n = 7$ qubit state can be computed exactly with approximately 10^5 -fold reduction in memory consumption. We have also proposed algorithms to incorporate the nature of the target quantum state, such as the permutation symmetry between multiple copies of states and the partially decoupled structure for inhomogeneous magic resources, and have numerically shown that we can scale the approximate RoM calculation up to $n = 17$ qubits.

Numerous future directions can be envisioned. First, it is intriguing to seek generalization to other quantum resource measures. Since the core subroutine in this work only assumes that the total system is composed of local systems with discrete degrees of freedom, we envision that our work can be applied to other resource monotones that are formulated with L^p norm optimization (in particular $p = 0, 1$) such as stabilizer extent [25], channel robustness [23], negativity [19]. In particular, it is nontrivial if we can extend the framework when the pure free states constitute a continuous set, such as in the case of fermionic non-Gaussianity [33, 34, 35]. Second, it is interesting to investigate whether it is possible to further scale up computations for weakly decoupled states such as tensor network states. While exact computation may require as costly calculation as in the generic case, we may perform approximate computation with an accuracy bound that depends on the entanglement.

Acknowledgements.— N.Y. wishes to thank JST PRESTO No. JPMJPR2119 and the support from IBM Quantum. This work was supported by JST Grant Number JP-MJPF2221. This work was supported by JST ERATO Grant Number JPMJER2302 and JST CREST Grant Number JPMJCR23I4, Japan.

References

- [1] Daniel Gottesman. “The Heisenberg Representation of Quantum Computers” (1998). [arxiv:quant-ph/9807006](https://arxiv.org/abs/quant-ph/9807006).
- [2] Michael A. Nielsen and Isaac L. Chuang. “Quantum Computation and Quantum Information: 10th Anniversary Edition”. [Cambridge University Press](https://www.cambridge.org/core/books/quantum-computation-and-quantum-information-10th-anniversary-edition/9780511976693). (2010).
- [3] Sergei Bravyi and Alexei Kitaev. “Universal Quantum Computation with ideal Clifford gates and noisy ancillas”. [Physical Review A **71**, 022316](https://doi.org/10.1103/PhysRevA.71.022316) (2005). [arxiv:quant-ph/0403025](https://arxiv.org/abs/quant-ph/0403025).
- [4] Daniel Litinski. “A Game of Surface Codes: Large-Scale Quantum Computing with Lattice Surgery”. [Quantum **3**, 128](https://doi.org/10.22331/q-2019-0620) (2019). [arxiv:1808.02892](https://arxiv.org/abs/1808.02892).
- [5] Dominic Horsman, Austin G. Fowler, Simon Devitt, and Rodney Van Meter. “Surface code quantum computing by lattice surgery”. [New Journal of Physics **14**, 123011](https://doi.org/10.1088/1367-2631/14/12/123011) (2012). [arxiv:1111.4022](https://arxiv.org/abs/1111.4022).
- [6] Austin G. Fowler and Craig Gidney. “Low overhead quantum computation using lattice surgery” (2019). [arxiv:1808.06709](https://arxiv.org/abs/1808.06709).
- [7] Craig Gidney and Martin Ekerå. “How to factor 2048 bit RSA integers in 8 hours using 20 million noisy qubits”. [Quantum **5**, 433](https://doi.org/10.22331/q-2021-0510) (2021).

[8] Joonho Lee, Dominic W. Berry, Craig Gidney, William J. Huggins, Jarrod R. McClean, Nathan Wiebe, and Ryan Babbush. “Even More Efficient Quantum Computations of Chemistry Through Tensor Hypercontraction”. *PRX Quantum* **2**, 030305 (2021).

[9] Vera von Burg, Guang Hao Low, Thomas Häner, Damian S. Steiger, Markus Reiher, Martin Roetteler, and Matthias Troyer. “Quantum computing enhanced computational catalysis”. *Physical Review Research* **3**, 033055 (2021).

[10] Nobuyuki Yoshioka, Tsuyoshi Okubo, Yasunari Suzuki, Yuki Koizumi, and Wataru Mizukami. “Hunting for quantum-classical crossover in condensed matter problems” (2023). [arxiv:2210.14109](https://arxiv.org/abs/2210.14109).

[11] Sergey Bravyi, Graeme Smith, and John Smolin. “Trading classical and quantum computational resources”. *Physical Review X* **6**, 021043 (2016). [arxiv:1506.01396](https://arxiv.org/abs/1506.01396).

[12] Emanuele Tirrito, Poetri Sonya Tarabunga, Gugliemo Lami, Titas Chanda, Lorenzo Leone, Salvatore F. E. Oliviero, Marcello Dalmonte, Mario Collura, and Alioscia Hamma. “Quantifying non-stabilizerness through entanglement spectrum flatness” (2023). [arxiv:2304.01175](https://arxiv.org/abs/2304.01175).

[13] Oliver Hahn, Alessandro Ferraro, Lina Hultquist, Giulia Ferrini, and Laura García-Álvarez. “Quantifying Qubit Magic Resource with Gottesman-Kitaev-Preskill Encoding”. *Physical Review Letters* **128**, 210502 (2022).

[14] Tobias Haug, Soovin Lee, and M. S. Kim. “Efficient stabilizer entropies for quantum computers” (2023). [arxiv:2305.19152](https://arxiv.org/abs/2305.19152).

[15] James R. Seddon, Bartosz Regula, Hakop Pashayan, Yingkai Ouyang, and Earl T. Campbell. “Quantifying Quantum Speedups: Improved Classical Simulation From Tighter Magic Monotones”. *PRX Quantum* **2**, 010345 (2021).

[16] Zi-Wen Liu and Andreas Winter. “Many-body quantum magic”. *PRX Quantum* **3**, 020333 (2022). [arxiv:2010.13817](https://arxiv.org/abs/2010.13817).

[17] Lorenzo Leone, Salvatore F. E. Oliviero, and Alioscia Hamma. “Stabilizer R\’enyi entropy”. *Physical Review Letters* **128**, 050402 (2022). [arxiv:2106.12587](https://arxiv.org/abs/2106.12587).

[18] Mark Howard and Earl T. Campbell. “Application of a resource theory for magic states to fault-tolerant quantum computing”. *Physical Review Letters* **118**, 090501 (2017). [arxiv:1609.07488](https://arxiv.org/abs/1609.07488).

[19] Hakop Pashayan, Joel J. Wallman, and Stephen D. Bartlett. “Estimating outcome probabilities of quantum circuits using quasiprobabilities”. *Physical Review Letters* **115**, 070501 (2015). [arxiv:1503.07525](https://arxiv.org/abs/1503.07525).

[20] Markus Heinrich and David Gross. “Robustness of Magic and Symmetries of the Stabiliser Polytope”. *Quantum* **3**, 132 (2019). [arxiv:1807.10296](https://arxiv.org/abs/1807.10296).

[21] Scott Aaronson and Daniel Gottesman. “Improved Simulation of Stabilizer Circuits”. *Physical Review A* **70**, 052328 (2004). [arxiv:quant-ph/0406196](https://arxiv.org/abs/quant-ph/0406196).

[22] Héctor J. García, Igor L. Markov, and Andrew W. Cross. “On the Geometry of Stabilizer States” (2017). [arxiv:1711.07848](https://arxiv.org/abs/1711.07848).

[23] James R. Seddon and Earl T. Campbell. “Quantifying magic for multi-qubit operations”. *Proceedings of the Royal Society A: Mathematical, Physical and Engineering Sciences* **475**, 20190251 (2019). [arxiv:1901.03322](https://arxiv.org/abs/1901.03322).

[24] Fino and Algazi. “Unified Matrix Treatment of the Fast Walsh-Hadamard Transform”. *IEEE Transactions on Computers* **C-25**, 1142–1146 (1976).

- [25] Sergey Bravyi, Dan Browne, Padraig Calpin, Earl Campbell, David Gosset, and Mark Howard. “Simulation of quantum circuits by low-rank stabilizer decompositions”. *Quantum* **3**, 181 (2019).
- [26] SciPy. “Scipy.sparse.csc_matrix — SciPy v1.11.2 Manual”. https://docs.scipy.org/doc/scipy/reference/generated/scipy.sparse.csc_matrix.html.
- [27] Hiroki Hamaguchi, Kou Hamada, and Nobuyuki Yoshioka. “Quantum-programming/RoM-handbook: Handbook for fast simulation of Robustness of Magic (RoM)”. <https://github.com/quantum-programming/RoM-handbook> (2023).
- [28] Gilbert Strang. “Linear algebra and learning from data”. Wellesley-Cambridge press. Wellesley (2019).
- [29] Michael Elad. “Sparse and Redundant Representations: From Theory to Applications in Signal and Image Processing”. *Springer*. New York, NY (2010).
- [30] David L. Donoho and Yaakov Tsaig. “Fast Solution of ℓ_1 -Norm Minimization Problems When the Solution May Be Sparse”. *IEEE Transactions on Information Theory* **54**, 4789–4812 (2008).
- [31] Guy Desaulniers, Jacques Desrosiers, and Marius M. Solomon, editors. “Column Generation”. *Springer US*. Boston, MA (2005).
- [32] Danielsen Lars Eirik. “Database of self-dual quantum codes”. <http://www.ii.uib.no/~larsed/vncorbits/>.
- [33] Beatriz Dias and Robert Koenig. “Classical simulation of non-Gaussian fermionic circuits” (2023). [arxiv:2307.12912](https://arxiv.org/abs/2307.12912).
- [34] Oliver Reardon-Smith, Michał Oszmaniec, and Kamil Korzekwa. “Improved simulation of quantum circuits dominated by free fermionic operations” (2023). [arxiv:2307.12702](https://arxiv.org/abs/2307.12702).
- [35] Joshua Cudby and Sergii Strelchuk. “Gaussian decomposition of magic states for matchgate computations” (2023). [arxiv:2307.12654](https://arxiv.org/abs/2307.12654).
- [36] G.I. Struchalin, Ya. A. Zagorovskii, E.V. Kovlakov, S.S. Straupe, and S.P. Kulik. “Experimental Estimation of Quantum State Properties from Classical Shadows”. *PRX Quantum* **2**, 010307 (2021).
- [37] Regina C. Elandt-Johnson and Norman L. Johnson. “Survival Models and Data Analysis”. *Wiley Series in Probability and Statistics*. Wiley. (1999). 1 edition.
- [38] Arno Jaeger and Bertram Mond. “On direct sums and tensor products of linear programs”. *Zeitschrift für Wahrscheinlichkeitstheorie und Verwandte Gebiete* **3**, 19–31 (1964).

A Pseudocode of fast Walsh–Hadamard transform algorithm

Here, we provide the pseudocode of the Fast Walsh–Hadamard Transform (FWHT) algorithm. Clearly, the in-place computation allows time complexity of $\mathcal{O}(n2^n)$ and the space complexity of $\mathcal{O}(2^n)$.

B Basic properties of inner product in Pauli vector representation

In this section, we provide a brief review of the basic properties of inner products in Pauli vector representation.

Algorithm 5: Fast Walsh–Hadamard Transform (FWHT) algorithm

Input: $v \in \mathbb{R}^{2^n}$
Output: In-place computation result of $H_n v$

```

1 Function FWHT( $v$ )
2    $h \leftarrow 1$ 
3   while  $h < \text{len}(v)$  do
4     for  $i \leftarrow 0$  to  $\text{len}(v) - 2h$  by  $2h$  do
5       for  $j \leftarrow i$  to  $i + h - 1$  do
6          $x \leftarrow v[j]$ 
7          $y \leftarrow v[j + h]$ 
8          $v[j] \leftarrow x + y$ 
9          $v[j + h] \leftarrow x - y$ 
10        end
11      end
12      // if normalize,  $v \leftarrow v/2$ 
13       $h \leftarrow 2h$ 
14   end

```

B.1 Complexity of computing Pauli vector representation

Let ρ be an n -qubit quantum state whose Pauli vector representation is given by $b_j = \text{Tr}[\rho P_j]$ where P_j is the j -th Pauli operator. In order to compute all the elements, naively the computational complexity scales as $\mathcal{O}(8^n)$ even if we use the sparse structure of each Pauli matrix. In the following, we show that we can perform an in-place computation that exponentially reduces the time complexity:

Lemma 4. (*Complexity of computing Pauli vector*) *Given the full density matrix representation of n -qubit quantum state ρ , its Pauli vector representation can be computed with time complexity of $\mathcal{O}(n4^n)$.*

Proof. First let us introduce a map from an n -qubit density matrix to a $2n$ -qubit statevector as follows:

$$\rho = \sum_{i,j} \rho_{i_1 \dots i_n, j_1 \dots j_n} |i_1 \dots i_n\rangle \langle j_1 \dots j_n| \mapsto \sum_{i,j} \rho_{i_1 \dots i_n, j_1 \dots j_n} |i_1, j_1, \dots, i_n, j_n\rangle. \quad (11)$$

Note that this is different from the well-known Choi map $\rho \mapsto \sum_{ij} \rho_{ij} |i\rangle |j\rangle$, and thus we refer to it as modified Choi vectorization. We introduce a modified Choi vector \mathbf{c} such that c_k denotes the k -th element, which can be obtained practically via extracting the matrix elements of ρ in the Z-order curve. Then, we find that \mathbf{c} is related with the Pauli vector representation \mathbf{b} as

$$\mathbf{b} = M_n \mathbf{c}, \quad (12)$$

where the transformation matrix M_n is defined as

$$M_n := M^{\otimes n}, \quad M := \begin{pmatrix} 1 & 0 & 0 & 1 \\ 0 & 1 & 1 & 0 \\ 0 & i & -i & 0 \\ 1 & 0 & 0 & -1 \end{pmatrix}. \quad (13)$$

Similar to the FWHT algorithm as provided in Algorithm 5, in-place computation for such a tensor-product structure can be done with time complexity of $\mathcal{O}(n4^n)$ and space complexity of $\mathcal{O}(4^n)$, which completes the proof. \square

B.2 Pauli vector overlap and quantum state fidelity

The fidelity between quantum states ρ_1 and ρ_2 is defined as

$$F(\rho_1, \rho_2) := \text{Tr} \left(\sqrt{\rho_1^{1/2} \rho_2 \rho_1^{1/2}} \right). \quad (14)$$

We can show that the fidelity is closely related to the Pauli vector as follows:

Lemma 5. *Let the Pauli vector representation of quantum states ρ_1 and ρ_2 be \mathbf{b}_1 and \mathbf{b}_2 , respectively. If at least one of ρ_1 and ρ_2 is a pure state, then the overlap $\frac{1}{2^n} \mathbf{b}_1^\top \mathbf{b}_2$ coincides with $F^2(\rho_1, \rho_2)$.*

Proof. It follows directly from the orthogonality of Pauli operators that $\frac{1}{2^n} \mathbf{b}_1^\top \mathbf{b}_2 = \text{Tr}[\rho_1 \rho_2]$. By taking $\rho_1 = |\psi\rangle\langle\psi|$ to be a pure state, we can show that $F^2(\rho_1, \rho_2) = \langle\psi|\rho_2|\psi\rangle = \text{Tr}[\rho_1 \rho_2]$. \square

It follows directly that the stabilizer fidelity can also be computed from the overlap computation between Pauli vectors. By denoting the Pauli vector of a pure stabilizer state $|\phi\rangle \in \mathcal{S}_n$ as \mathbf{b}_ϕ , we can show the following:

Corollary 2. *(Stabilizer fidelity as Pauli vector inner product) Let $\rho = |\psi\rangle\langle\psi|$ be a pure state with its Pauli vector given as \mathbf{b}_ρ . Then,*

$$\frac{1}{2^n} \left(\max_{|\phi\rangle \in \mathcal{S}_n} \mathbf{b}_\rho^\top \mathbf{b}_\phi \right) = \max_{|\phi\rangle \in \mathcal{S}_n} |\langle\phi|\psi\rangle|^2 = F_{\text{STAB}}(|\psi\rangle). \quad (15)$$

Finally, we provide a fact that is useful as a preknowledge regarding the distribution of overlaps in addition to the fact that $0 \leq \mathbf{b}_\rho^\top \mathbf{b}_\phi \leq 2^n$.

Lemma 6. *(Bound on overlap counts) Let ρ be an arbitrary n -qubit quantum state. Then, for all $n \in \mathbb{N}$, the count on the pure stabilizer states satisfies the following:*

$$\#\{\phi_- \in \mathcal{S}_n \mid \mathbf{b}_\rho^\top \mathbf{b}_{\phi_-} \in [0, 1]\} \geq |\mathcal{S}_n|/2^n, \quad (16)$$

$$\#\{\phi_+ \in \mathcal{S}_n \mid \mathbf{b}_\rho^\top \mathbf{b}_{\phi_+} \in [1, 2^n]\} \geq |\mathcal{S}_n|/2^n. \quad (17)$$

Proof. Let us take an arbitrary $\phi \in \mathcal{S}_n$, and consider a set Φ of 2^n stabilizer states whose stabilizer generators are equivalent to ϕ except for their signs. Then, it holds that

$$\sum_{\hat{\phi} \in \Phi} \mathbf{b}_\rho^\top \mathbf{b}_{\hat{\phi}} = 2^n. \quad (18)$$

Therefore, if we assume that the overlap is either all $\mathbf{b}_\rho^\top \mathbf{b}_{\hat{\phi}} < 1$ or all $\mathbf{b}_\rho^\top \mathbf{b}_{\hat{\phi}} > 1$, then this contradicts with Eq. (18), which completes the proof. \square

C Check matrix representation

One of the most well-known concise representations of a stabilizer state is the stabilizer tableau [21], which uses binary representation and the sign of each stabilizer generator. Meanwhile, in order to certify if a given set of Pauli operators suffices as an n -qubit stabilizer group generators, we may neglect the sign information and focus only on the commutativity and linear independence of generators. Here, we briefly introduce the check matrix representation [2] for the sake of convenience in discussion of Appendix D and E.

Let an n -qubit stabilizer group be given as $\langle g_1, \dots, g_n \rangle$ so that $-I^{\otimes n}$ is not included as an element. Let each generator be expressed in the binary symplectic form as

$$g_i = (-1)^{\chi_i} X_i^{\alpha_i} Z^{\beta_i}, \quad (19)$$

where $X^{\alpha_i} := X^{\alpha_{i,1}} \otimes \dots \otimes X^{\alpha_{i,n}}$ ($\alpha_{i,j} \in \{0, 1\}$), $Z^{\beta_i} := Z^{\beta_{i,1}} \otimes \dots \otimes Z^{\beta_{i,n}}$ ($\beta_j \in \{0, 1\}$), and $\chi_i \in \{0, 1\}$. The check matrix representation of the stabilizer group is given as $n \times 2n$ matrix as

$$\mathbf{C} = [\mathbf{X} \ \mathbf{Z}], \quad (20)$$

where $(\mathbf{X})_{i,j} = \alpha_{i,j}$ and $(\mathbf{Z})_{i,j} = \beta_{i,j}$ denote the (i, j) elements of the left and right half of the check matrix, respectively. Note that such a representation is unique except for the degrees of signs. Using the check matrix representation, we may confirm the linear independence and the commutativity of stabilizer generators. Such useful properties can be summarized as follows:

Lemma 7. *(Linear independence of stabilizer generators, Proposition 10.3 of Ref. [2])* The generators of a stabilizer group are mutually independent if and only if the rows of the corresponding check matrix \mathbf{C} are linearly independent, i.e., full row rank.

Lemma 8. *(Commutativity of stabilizer generators)* Let $G = \{g_1, \dots, g_n\}$ be a set of n -qubit stabilizer generators and \mathbf{C} be the check matrix corresponding to G . Then, the following two conditions are equivalent:

$$(i) \ [g_i, g_j] = 0 \text{ for all } g_i, g_j \in G.$$

$$(ii) \ \mathbf{C} \begin{pmatrix} O & I_n \\ I_n & O \end{pmatrix} \mathbf{C}^\top = 0.$$

Note that the operations for the check matrix are done modulo two.

D Proof of Lemma 2

Here we prove Lemma 2 in the main text that states that \mathbf{A}_n can be decomposed into sparsified Walsh–Hadamard matrices.

Lemma 9. *(Restatement of Lemma 2 in the main text)* For all $n \in \mathbb{N}$, there exists a constructive and efficient way of enumerating properly sparsified Walsh–Hadamard matrices $\{W_j\}_{j=1}^{|\mathcal{S}_n|/2^n}$ ($W_j \in \mathcal{W}_n$) such that

$$\mathbf{A}_n = [W_1 \cdots W_{|\mathcal{S}_n|/2^n}]. \quad (21)$$

Proof. Recall that, any set of n -qubit stabilizer generators $\{g_i\}_{i=1}^n$ can be related to other $2^n - 1$ stabilizer states by considering a state corresponding to $\{(-1)^{\chi_i} g_i\}_{i=1}^n$. This implies that a single check matrix corresponds to 2^n stabilizer states; thus, a check matrix yields a sparsified Walsh–Hadamard matrix.

Next, we show that there is a constructive and efficient way to enumerate all the check matrices using a standard form that allows the unique description of a check matrix. While some standard forms suffice for such a purpose, here we employ the following standard form:

$$\left(\begin{array}{cc|cc} I_k & X_1 & Z_1 & O \\ O & O & X_1^\top & I_{n-k} \end{array} \right), \quad (22)$$

where $X_1 \in \mathbb{F}_2^{k \times (n-k)}$ is given by reduced row echelon form of rank k and $Z_1 = Z_1^\top \in \mathbb{F}_2^{k \times k}$ is a symmetric matrix. Since all the choices of X_1 and Z_1 give rise to mutually different check matrices that satisfy both Lemmas 7 and 8, we can assure that Eq. (22) yields a unique and complete construction of the entire set of check matrix. \square

We remark that we can check the validity of the above construction by computing the total number of check matrices. The number of choices for Z_1 is $2^{k(k+1)/2}$ while the number of choices for X_1 is given by the q -binomial coefficient $\begin{bmatrix} n \\ k \end{bmatrix}_q$, which is defined for general $q (\neq 1)$ as

$$\begin{bmatrix} n \\ k \end{bmatrix}_q = \frac{(1-q^n)(1-q^{n-1})\dots(1-q^{n-k+1})}{(1-q)(1-q^2)\dots(1-q^k)}. \quad (23)$$

Therefore, by using $\sum_{k=0}^n \begin{bmatrix} n \\ k \end{bmatrix}_q 2^{k(k+1)/2} = |\mathcal{S}_n|/2^n$ which can be derived from the q -binomial theorem [36], we can certify the validity.

E Proof of Proposition 1

In this section, we provide the proof for Proposition 1 regarding the existence of the cover stabilizer set.

Proposition 3. (Restatement of Proposition 1 in the main text) *Let S_n be a subset of \mathcal{S}_n such that, for any $P \in \mathcal{P}_n$ there exists $|\psi\rangle \in S_n$ that satisfies $\{P, -P\} \cap \text{Stab}(|\psi\rangle) \neq \emptyset$. Then, for all $n \in \mathbb{N}$, the size of the set is bounded as $|S_n| \geq 2^n + 1$, and one can construct S_n such that $|S_n| = 2^n + 1$.*

E.1 Main proof

E.1.1 Proof on size bound

First we show that $|S_n| \geq 2^n + 1$. Note that $I^{\otimes n} \in \text{Stab}(|\psi\rangle)$ holds for any $|\psi\rangle \in S_n$, and therefore $\text{Stab}(|\psi\rangle) \setminus \{I^{\otimes n}\}$ consists of $2^n - 1$ elements. Therefore, in order to cover the remaining $4^n - 1$ elements of $\{I, X, Y, Z\}^{\otimes n} \setminus \{I^{\otimes n}\}$, the number of stabilizers satisfies

$$|S_n| \geq (4^n - 1)/(2^n - 1) = 2^n + 1. \quad (24)$$

E.1.2 Proof on the existence of minimum cover stabilizer set

Next, we prove the latter half of Proposition 3 that, there exists a cover stabilizer set S_n such that $|S_n| = 2^n + 1$. In the following, we explicitly construct S_n with $|S_n| = 2^n + 1$, and show that S_n satisfies the desired properties. Note that the overall sign of the stabilizer generators in the following argument is not relevant, and hence not discussed explicitly.

Let us take $|+\rangle^{\otimes n}$ as the 0-th element for S_n . For the k -th element ($1 \leq k \leq 2^n$), we take a state whose check matrix $\mathbf{C}_k = [\mathbf{X}_k \ \mathbf{Z}_k]$ is given as follows:

1. \mathbf{Z}_k is an $n \times n$ identity matrix.
2. \mathbf{X}_k is given such that Lemma 10 is satisfied.

Lemma 10. *There exists an explicit construction for a set of symmetric matrices $\{\mathbf{X}_k \mid \mathbf{X}_k \in \mathbb{F}_2^{n \times n}\}_{k=1}^{2^n}$ such that the following is satisfied.*

$$\forall \mathbf{v} \in \mathbb{F}_2^n \setminus \{\mathbf{0}\}, \ \{\mathbf{X}_k \mathbf{v}\}_{k=1}^{2^n} = \mathbb{F}_2^n. \quad (25)$$

From the fact that \mathbf{X}_k are all symmetric matrices, it follows that the condition in Lemma 8 is satisfied, and therefore $\mathbf{C}_k = [\mathbf{X}_k \ \mathbf{Z}_k]$ indeed yields a valid representation of some pure stabilizer state.

Let us show that the constructed S_n indeed satisfies the condition in Proposition 3. Since it is obvious that $P \in \{I, X\}^{\otimes n}$ is covered by $|+\rangle^{\otimes n}$, we focus on other Pauli operators that are denoted as $P = (-1)^\chi X^\alpha Z^\beta$ with $\beta \neq 0$.

Consider some state $|\psi_k\rangle$ whose check matrix is given by \mathbf{X}_k and \mathbf{Z}_k . For any $\mathbf{f} \in \mathbb{F}_2^n$, we can take $P_{k,\mathbf{f}} \in \{I, X, Y, Z\}^{\otimes n}$ so that its binary symplectic form yields $P_{k,\mathbf{f}} \approx X^{\mathbf{X}_k \mathbf{f}} Z^{\mathbf{Z}_k \mathbf{f}}$, and thus $\{P_{k,\mathbf{f}}, -P_{k,\mathbf{f}}\} \cap \text{Stab}(|\psi_k\rangle) \neq \emptyset$.

Now let us take $\mathbf{f} = \beta$. Due to Lemma 10, we can take k such that $\mathbf{X}_k \beta = \alpha$. This implies that the X and Z exponents of binary symplectic form of $P_{k,\mathbf{f}}$ can be given as $\mathbf{X}_k \mathbf{f} = \alpha$ and $\mathbf{Z}_k \mathbf{f} = \beta$, respectively. This implies $P_{k,\mathbf{f}} = P$ so that $\{P, -P\} \cap \text{Stab}(|\psi_k\rangle) \neq \emptyset$, and therefore satisfies the condition of Proposition 3.

E.2 Proof of Technical Lemma 10

Now the remaining work is to prove Lemma 10. We first provide the explicit construction of $\{\mathbf{X}_k\}_{k=1}^{2^n}$, and then prove that it indeed satisfies Eq. (25).

E.2.1 Construction of \mathbf{X}_k

We first introduce some algebraic concepts necessary for the discussion. We denote the polynomial ring over \mathbb{F}_2 by $\mathbb{F}_2[x]$. Let f be an arbitrary irreducible polynomial of degree n . We consider a quotient ring $\mathbb{F}_2[x]/(f)$, where (f) denotes the ideal generated by f . Then, $\mathbb{F}_2[x]/(f)$ is a field because f is irreducible. It is also noteworthy that $\mathbb{F}_2[x]/(f)$ is a vector space over \mathbb{F}_2 and $\{x^0, \dots, x^{n-1}\}$ can be taken as a basis.

In what follows, we discuss the construction of $\{\mathbf{X}_k\}_{k=1}^{2^n}$. We define a symmetric matrix $C(x) \in (\mathbb{F}_2[x]/(f))^{n \times n}$ as a matrix whose (i, j) entry equals x^{i+j-2} . Namely, $C(x)$ can be represented as follows:

$$C(x) = \begin{pmatrix} x^0 & x^1 & x^2 & \dots & x^{n-1} \\ x^1 & x^2 & & & \\ x^2 & & \ddots & & \vdots \\ \vdots & & & & \\ x^{n-1} & & \dots & & x^{2n-2} \end{pmatrix}.$$

Every entry of $C(x)$ can be represented as a linear combination of a basis $\{x^0, \dots, x^{n-1}\}$, and we define C_i be a matrix consisting of such x^i coefficients. In other words, $C_i \in \mathbb{F}_2^{n \times n}$ is defined so that $C(x) = C_0 x^0 + \dots + C_{n-1} x^{n-1}$ holds. Note that C_i is also symmetric.

We give a concrete example below. We take $n = 3$ and $f = 1 + x + x^3$, which is

irreducible. Then, C_0, C_1, C_2 can be derived in the following way:

$$\begin{aligned}
C(x) &= \begin{pmatrix} x^0 & x^1 & x^2 \\ x^1 & x^2 & x^3 \\ x^2 & x^3 & x^4 \end{pmatrix} \\
&= \begin{pmatrix} 1 & x & x^2 \\ x & x^2 & 1+x \\ x^2 & 1+x & x+x^2 \end{pmatrix} \\
&= \underbrace{\begin{pmatrix} 1 & & \\ & 1 \end{pmatrix}}_{C_0} x^0 + \underbrace{\begin{pmatrix} 1 & & \\ & 1 & 1 \\ & 1 & 1 \end{pmatrix}}_{C_1} x^1 + \underbrace{\begin{pmatrix} 1 & & \\ & 1 & 1 \\ & 1 & 1 \end{pmatrix}}_{C_2} x^2.
\end{aligned}$$

Next, we consider the following set of symmetric matrices:

$$\left\{ \sum_{i=0}^{n-1} a_i C_i \mid a_i \in \mathbb{F}_2 \right\}.$$

Since the elements of the set are distinct, the set has 2^n elements. We take this set as the set $\{\mathbf{X}_k\}_{k=1}^{2^n}$.

E.2.2 Proof that \mathbf{X}_k satisfies Lemma 10

Next, we prove that $\{\mathbf{X}_k\}_{k=1}^{2^n}$ given in the previous subsection satisfies Eq. (25).

By the definition of \mathbf{X}_k , one can show that Eq. (25) holds if and only if $\{C_i \mathbf{v}\}_{i=0}^{n-1}$ is linearly independent for any $\mathbf{v} \in \mathbb{F}_2^n \setminus \{\mathbf{0}\}$. From here, we show the linear independence of $\{C_i \mathbf{v}\}_{i=0}^{n-1}$ by proving several lemmas.

Lemma 11. *For any vectors $\mathbf{u}, \mathbf{v} \in \mathbb{F}_2^n \setminus \{\mathbf{0}\}$, $\mathbf{u}^\top C(x) \mathbf{v} \neq 0$.*

Proof. Using a vector $\mathbf{x} = (x^0, \dots, x^{n-1})^\top$, we have $C(x) = \mathbf{x} \mathbf{x}^\top$. Thus, by defining two polynomials $u(x) = \mathbf{u}^\top \mathbf{x} = \sum_{i=0}^{n-1} u_i x^i$ and $v(x) = \mathbf{v}^\top \mathbf{x} = \sum_{i=0}^{n-1} v_i x^i$, $\mathbf{u}^\top C(x) \mathbf{v}$ can be represented as $u(x)v(x)$. Hence, it suffices to show that $u(x)v(x) \neq 0$. Because \mathbf{u} and \mathbf{v} are nonzero, $u(x)$ and $v(x)$ are nonzero as well. Noting that $\mathbb{F}_2/(f)$ is a field, the product $u(x)v(x)$ is also nonzero. \square

Lemma 12. *For any vectors $\mathbf{u}, \mathbf{v} \in \mathbb{F}_2^n \setminus \{\mathbf{0}\}$, there exists i such that $\mathbf{u}^\top C_i \mathbf{v} \neq 0$.*

Proof. By multiplying $C(x) = C_0 x^0 + \dots + C_{n-1} x^{n-1}$ by \mathbf{u} from the left and \mathbf{v} from the right, we obtain

$$\mathbf{u}^\top C(x) \mathbf{v} = (\mathbf{u}^\top C_0 \mathbf{v}) x^0 + \dots + (\mathbf{u}^\top C_{n-1} \mathbf{v}) x^{n-1}. \quad (26)$$

Eq. (26) expresses $\mathbf{u}^\top C(x) \mathbf{v}$ as a polynomial with coefficients $\mathbf{u}^\top C_i \mathbf{v} \in \mathbb{F}_2$. Since $\mathbf{u}^\top C(x) \mathbf{v}$ is nonzero from Lemma 11, there exists a nonzero coefficient, i.e., $\mathbf{u}^\top C_i \mathbf{v} \neq 0$ for some i . \square

Lemma 13. *For any vector $\mathbf{v} \in \mathbb{F}_2^n \setminus \{\mathbf{0}\}$, $\{C_i \mathbf{v}\}_{i=0}^{n-1}$ is linearly independent.*

Proof. We consider a matrix $[C_0 \mathbf{v}, \dots, C_{n-1} \mathbf{v}]$ with $C_i \mathbf{v}$ as the column vectors. By multiplying an arbitrary nonzero vector $\mathbf{u} \in \mathbb{F}_2^n \setminus \{\mathbf{0}\}$ from the left, we obtain a vector $(\mathbf{u}^\top C_0 \mathbf{v}, \dots, \mathbf{u}^\top C_{n-1} \mathbf{v})$, which is nonzero by Lemma 12. Therefore, we can confirm that the matrix $[C_0 \mathbf{v}, \dots, C_{n-1} \mathbf{v}]$ is non-singular, which implies the linear independence of $\{C_i \mathbf{v}\}_{i=0}^{n-1}$. \square

Having shown Lemma 13, it is also proved that $\{\mathbf{X}_k\}_{k=1}^{2^n}$ given in the previous subsection satisfies Eq. (25), i.e., Lemma 10 is proved.

F Proof of Lemma 3

In this section, we prove Lemma 3 in the main text, which provides the accuracy bound on the minimal feasible solution for RoM calculation. Let us first recall that the Pauli vector \mathbf{b} of length- 4^n is decomposed in correspondence with the minimal cover matrix as $\{\mathbf{b}_i\}_{i=1}^{2^n+1}$ where each \mathbf{b}_i is a length- 2^n vector. The Lemma 3 is based on the observation that \mathbf{b}_i seems to obey normal distribution for random states. This motivates us to show the random average of the approximate value R_{FWHT} as follows.

Lemma 14. (Restatement of Lemma 3) *Let \mathbf{b}_i drawn uniformly from $\mathcal{N}(\mathbf{0}, \mathbf{I})$ for all j . Then,*

$$\mathbb{E}_{\mathbf{b}_i \sim \mathcal{N}(\mathbf{0}, \mathbf{I})} \left[\frac{R_{\text{FWHT}}}{\|\rho\|_{\text{st}}} \right] \approx 2^{n/2}. \quad (27)$$

Proof. Recall that the FWHT algorithm for i -th segment \mathbf{b}_i yields the segment of minimal feasible solution \mathbf{x}_i , from which the approximate RoM value is obtained as

$$R_{\text{FWHT}} = \sum_{i=1}^{2^n+1} \|\mathbf{x}_i\|_1 = \frac{1}{2^n} \sum_{i=1}^{2^n+1} \|H_n \mathbf{b}_i\|_1. \quad (28)$$

By combining with the definition of the st-norm $\|\rho\|_{\text{st}} = \frac{1}{2^n} \|\mathbf{b}\|_1 = \frac{1}{2^n} \sum_{i=1}^{2^n+1} \|\mathbf{b}_i\|_1$, we obtain

$$\begin{aligned} \mathbb{E}_{\mathbf{b}_i \sim \mathcal{N}(\mathbf{0}, \mathbf{I})} \left[\frac{R_{\text{FWHT}}}{\|\rho\|_{\text{st}}} \right] &= \mathbb{E}_{\mathbf{b}_i \sim \mathcal{N}(\mathbf{0}, \mathbf{I})} \left[\frac{\sum_{i=1}^{2^n+1} \|H_n \mathbf{b}_i\|_1}{\sum_{i=1}^{2^n+1} \|\mathbf{b}_i\|_1} \right] \\ &= \sum_{i=1}^{2^n+1} 2^n \mathbb{E}_{\mathbf{b}_i \sim \mathcal{N}(\mathbf{0}, \mathbf{I})} \left[\frac{|\mathbf{1}^\top \mathbf{b}_i|}{\sum_{i=1}^{2^n+1} \|\mathbf{b}_i\|_1} \right] \\ &= 2^n \mathbb{E}_{b_{ij} \sim \mathcal{N}(0, 1)} \left[\frac{\sum_{i=1}^{2^n+1} \left| \sum_{j=1}^{2^n} b_{ij} \right|}{\sum_{i=1}^{2^n+1} \sum_{j=1}^{2^n} |b_{ij}|} \right], \end{aligned} \quad (29)$$

where, to derive the second equation, we have used the fact the matrix elements of the Walsh–Hadamard matrix H_n only consist of ± 1 and that the elements of \mathbf{b}_i are distributed symmetrically with respect to sign change. We have also denoted the elements of the vector as $\mathbf{b}_i = (\dots, b_{ij}, \dots)$.

In order to evaluate Eq. (29), we utilize the second order formula for random variable as [37]

$$\mathbb{E}\left[\frac{X}{Y}\right] \approx \frac{\mathbb{E}[X]}{\mathbb{E}[Y]} - \frac{\text{Cov}(X, Y)}{\mathbb{E}[Y]^2} + \frac{\text{Var}(Y)\mathbb{E}[X]}{\mathbb{E}[Y]^3}. \quad (30)$$

It can be shown that $X = \sum_{i=1}^{2^n+1} \left| \sum_{j=1}^{2^n} b_{ij} \right|$, $Y = \sum_{i=1}^{2^n+1} \sum_{j=1}^{2^n} |b_{ij}|$ can be evaluated as

$$\frac{\mathbb{E}[X]}{\mathbb{E}[Y]} = \frac{1}{2^{n/2}}, \quad \frac{\text{Cov}(X, Y)}{\mathbb{E}[Y]^2} = o\left(\frac{1}{2^n}\right), \quad \frac{\text{Var}(Y)\mathbb{E}[X]}{\mathbb{E}[Y]^3} = o\left(\frac{1}{2^n}\right). \quad (31)$$

Therefore, by substituting this into Eq. (30), we finally obtain

$$2^n \mathbb{E}\left[\frac{X}{Y}\right] \approx 2^{n/2} + o(1),$$

which completes the proof. \square

While the Lemma holds for asymptotically large n , we numerically find that the convergence is observed for moderate n . Namely, we have numerically computed the values for 100 random 10-qubit mixed states to show that

$$\left(\frac{R_{\text{FWHT}}}{\|\rho\|_{\text{st}}} \right)^{\frac{1}{n}} = 1.41412 \pm 0.00006. \quad (32)$$

This implies that we can readily expect the accuracy bound to hold in moderate-size systems.

G Proof of Proposition 2

In this section, we prove Proposition 2 which assures that when one restricts the pure stabilizer sets so that the target problem is described by tensor product as $\bigotimes_i \mathbf{A}_{n_i} \subset \mathbf{A}_n$, the solution is simply a tensor product of individual solution. The proof can be similarly done by following arguments provided in Ref. [38].

Let us consider a general L^1 norm minimization problem with a tensor product structure over M subsystems as

$$\begin{aligned} (\mathbf{P}) \text{ minimize}_{\mathbf{x}} \quad & \|\mathbf{x}\|_1 \\ \text{subject to} \quad & \left(\bigotimes_{i=1}^M \mathbf{A}_i \right) \mathbf{x} = \bigotimes_{i=1}^M \mathbf{b}_i, \end{aligned}$$

where the i -th subsystem can be formulated as

$$\begin{aligned} (\mathbf{P}_i) \text{ minimize}_{\mathbf{x}_i} \quad & \|\mathbf{x}_i\|_1 \\ \text{subject to} \quad & \mathbf{A}_i \mathbf{x}_i = \mathbf{b}_i. \end{aligned}$$

Assuming that optimal solution exists for every (\mathbf{P}_i) , the following holds.

Lemma 15. *Let \mathbf{x}_i^* be the optimal solution for (\mathbf{P}_i) . Then, $\mathbf{x}^* = \bigotimes_{i=1}^M \mathbf{x}_i^*$ is the optimal solution for (\mathbf{P}) .*

Proof. It is obvious that \mathbf{x}^* is a feasible solution, and therefore we show the optimality of \mathbf{x}^* via duality. The dual problem for the total system is given as

$$\begin{aligned} (\mathbf{D}) \text{ maximize}_{\mathbf{y}} \quad & \left(\bigotimes_{i=1}^M \mathbf{b}_i^\top \right) \mathbf{y} \\ \text{subject to} \quad & \left\| \left(\bigotimes_{i=1}^M \mathbf{A}_i^\top \right) \mathbf{y} \right\|_\infty \leq 1. \end{aligned}$$

where the dual problem for each subsystem can also be provided as

$$\begin{aligned} (\mathbf{D}_i) \text{ maximize}_{\mathbf{y}_i} \quad & \mathbf{b}_i^\top \mathbf{y}_i \\ \text{subject to} \quad & \left\| \mathbf{A}_i^\top \mathbf{y}_i \right\|_\infty \leq 1. \end{aligned}$$

Now the strong duality of the problem assures that optimal solution \mathbf{y}_i^* exists for any (\mathbf{D}_i) with the optimal value given as $\|\mathbf{x}_i^*\|_1 = \mathbf{b}_i^\top \mathbf{y}_i^*$. By taking $\mathbf{y}^* := \bigotimes_{i=1}^M \mathbf{y}_i^*$, then it follows from the property of L^∞ norm that

$$\left\| \left(\bigotimes_{i=1}^M \mathbf{A}_i^\top \right) \mathbf{y}^* \right\|_\infty = \left\| \bigotimes_{i=1}^M \left(\mathbf{A}_i^\top \mathbf{y}_i^* \right) \right\|_\infty = \prod_{i=1}^M \left\| \mathbf{A}_i^\top \mathbf{y}_i^* \right\|_\infty \leq 1,$$

which guarantees that \mathbf{y}^* is a feasible solution of (D). Now the objective function for the dual problem (D) satisfies

$$\left(\bigotimes_{i=1}^M \mathbf{b}_i^\top \right) \mathbf{y}^* = \prod_{i=1}^M \left(\mathbf{b}_i^\top \mathbf{y}_i^* \right) = \prod_{i=1}^M \|\mathbf{x}_i^*\|_1 = \left\| \bigotimes_{i=1}^M \mathbf{x}_i^* \right\|_1 = \|\mathbf{x}^*\|_1. \quad (33)$$

Therefore, the objective functions of feasible solutions \mathbf{x}^* and \mathbf{y}^* for the primal and dual problems coincide with each other and hence are optimal due to the strong duality. \square

Given Lemma 15, Proposition 2 in the main text follows directly by applying to the calculation of RoM.

H Numerical details on RoM calculation

In this section, we provide details on the numerical results on RoM calculation.

H.1 More results on top-overlap method

Here, we provide the results on numerical demonstration regarding the top-overlap method introduced in Sec. 3.2 in the main text. Concretely, we present results for random mixed, pure, tensor product states of $n = 4, 5, 6, 7$ qubit system.

As is shown in Fig. 9, we can see that the top-overlap method significantly outperforms naive random selection methods in all cases. We can see that the improvement becomes more evident when we simulate larger systems; in particular, for $n = 7$ qubit case it suffices to take only $K = 10^{-5}$ to reach near-optimal value for any target.

Two remarks are in order. First, we note that we have added the column set of cover matrix in the case of tensor product states, in order to assure the existence of a feasible solution. In other words, the restriction of the column set solely using the information of overlaps may lead to rank deficient matrix. Second, the run time of our algorithm for the $n = 6$ qubit system was approximately 5 seconds for computing all the overlaps and 3 minutes for solving the LP. For the case of the $n = 7$ qubit system, the overlap computation consumes 15 minutes at most and 15 minutes for solving the LP. The simulation was done on a single laptop, and we envision that the use of MPI or GPU shall further speed up the computation.

H.2 Assuring feasibility

As mentioned in the previous subsection, we cannot obtain any feasible solution if the set of stabilizer states are not appropriately restricted.

One of the most robust ways to assure feasibility for arbitrary quantum states is to utilize an efficiently computed approximate solution with relatively low precision. Formally, we can understand this as modifying the problem as

$$\begin{aligned} & \underset{\mathbf{x}}{\text{minimize}} && \|\mathbf{x}\|_1 + c\|\mathbf{e}\|_1 \\ & \text{subject to} && \mathbf{A}\mathbf{x} - \mathbf{b} = \mathbf{e}, \end{aligned} \quad (34)$$

where \mathbf{e} is introduced to absorb the numerical error due to rank deficiency, and c is a hyperparameter that determines the penalty due to such an error. In practice, one may add the cover matrix to the set of stabilizers for such a purpose.

The second method that is applicable in the case of tensor product states is to utilize the solution obtained from small scale systems. As shown in Lemma 15 in Appendix G,

we can always obtain a feasible solution by taking tensor products and hence can be used as an initialization. Therefore, one may extend the set of stabilizers so that the quality of the solution is improved. Such a technique is also valid for the Column Generation method presented in Sec. 4.

H.3 Overlap computation using singular value decomposition

Here, we discuss how to efficiently compute the overlap between the Pauli vector \mathbf{b} of $(n+m)$ -qubit system and a stabilizer state that can be decomposed into a tensor product of n and m -qubit stabilizer state.

First, let us consider singular value decomposition of the Pauli vector as $\mathbf{b} = \sum_{k=1}^r \sigma_k (u_k \otimes v_k)$ where r is the number of nonzero singular values, u_k and v_k is the k -th vector of n and m -qubit system with singular value of σ_k . Then, the overlap with all stabilizer states in $\mathcal{S}_n \otimes \mathcal{S}_m$ ($\subset \mathcal{S}_{n+m}$) can be computed efficiently by noting that

$$\mathbf{b}^\top (\mathbf{A}_n \otimes \mathbf{A}_m) = \sum_{k=1}^r \sigma_k ((u_k^\top \mathbf{A}_n) \otimes (v_k^\top \mathbf{A}_m)) \quad (35)$$

$$= \text{vec}(U^\top V), \quad (36)$$

where ‘‘vec’’ denotes the vectorization of a matrix, U and V are matrices whose k -th row are given as $\sqrt{\sigma_k} u_k^\top \mathbf{A}_n$ and $\sqrt{\sigma_k} v_k^\top \mathbf{A}_m$, respectively. From Eq. (35) to Eq. (36), we have utilized the tensor product structure as

$$\left(\sum_k \boldsymbol{\lambda}^{(k)} \otimes \boldsymbol{\xi}^{(k)} \right)_{(l,m)} = \sum_k \lambda_l^{(k)} \xi_m^{(k)} = (\Lambda^\top \Xi)_{l,m} = \text{vec}(\Lambda^\top \Xi), \quad (37)$$

where $\Lambda = (\dots, \boldsymbol{\lambda}^{(k)}, \dots)$ and $\Xi = (\dots, \boldsymbol{\xi}^{(k)}, \dots)$.

The matrix-matrix product in Eq. (36) can be computed with time complexity of $\mathcal{O}(r(n|\mathcal{S}_n| + m|\mathcal{S}_m| + |\mathcal{S}_n||\mathcal{S}_m|))$. In particular, when the target state is completely decoupled into two subsystems as $r = 1$, then the maximal value of all the overlaps between $|\mathcal{S}_n||\mathcal{S}_m|$ states can be computed with time complexity of $\mathcal{O}(n|\mathcal{S}_n| + m|\mathcal{S}_m|)$.

Note that, the above technique can be utilized as an initialization technique. Namely, one may discard small singular values so that we can perform data compression as long as the truncated state well-reproduces the original target state. Given the compressed data, we have used the Khatri-Rao product to regenerate the columns in $n+m$ -qubit system. In this sense, one may further extend the approximation algorithm to low-entangled states that can be represented efficiently by, e.g., tensor networks.

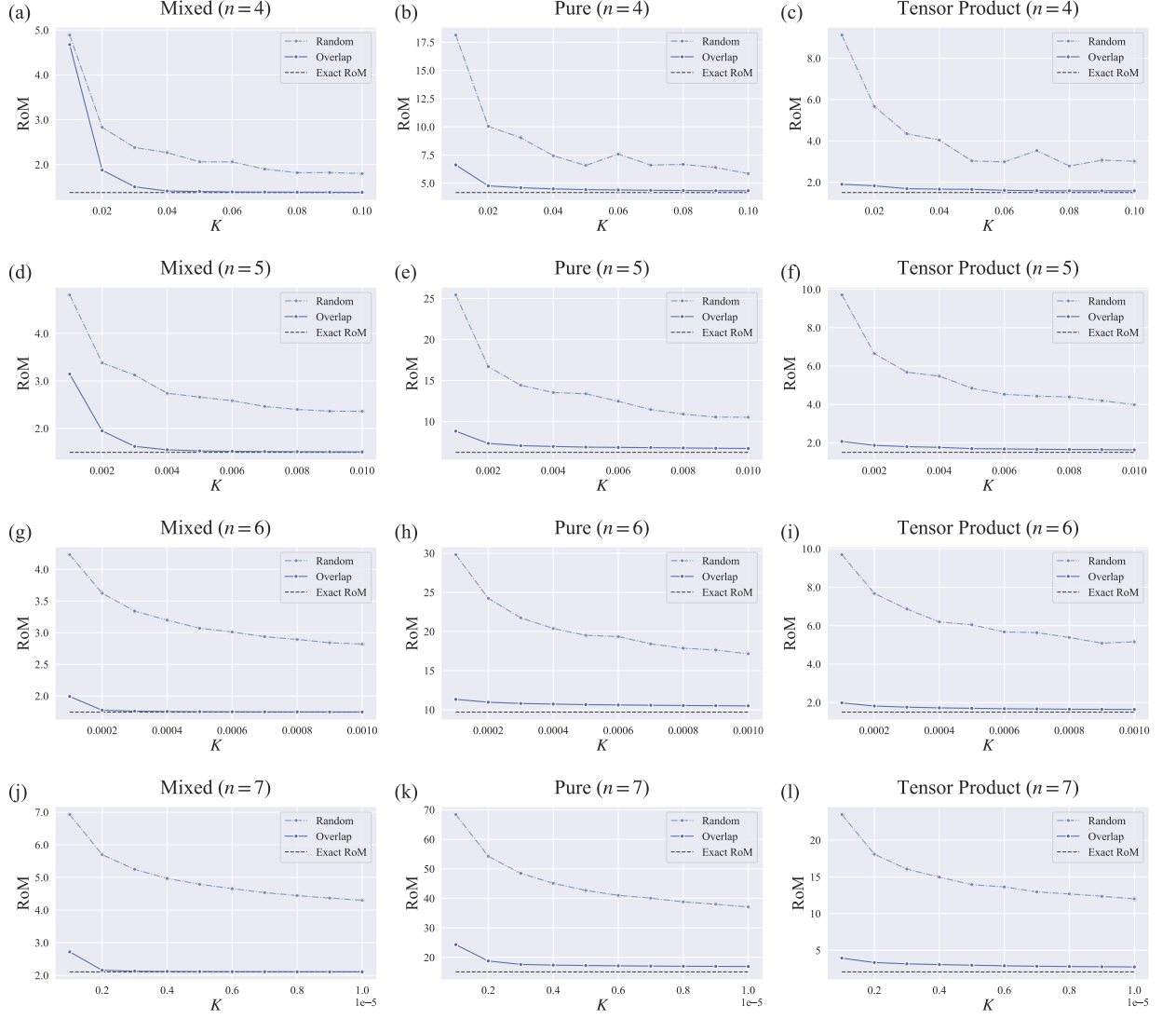


Figure 9: Numerical demonstration of top-overlap method introduced in Sec. 3.2 in the main text. The column set is restricted to $K|\mathcal{S}_n|$ ($0 < K \leq 1$). The cyan and blue lines denote the approximate RoM values computed by restricting the column set of stabilizers at random and by taking the largest and smallest overlaps, respectively. The black dotted lines indicate the exact RoM values which is computed with Column Generation method.